NOTICE

CERTAIN DATA CONTAINED IN THIS DOCUMENT MAY BE DIFFICULT TO READ IN MICROFICHE PRODUCTS.

CONF-900944--31

DE91 006552

CHARACTERIZATION OF COMPOSITE HIGH TEMPERATURE SUPERCONDUCTORS FOR MAGNETIC BEARING APPLICATIONS

by

B. R. Weinberger, L. Lynds, J. VanValzah, and H. Eaton
United Technologies Research Center
East Hartford, Connecticut 06108

and

J. R. Hull, T. M. Mulcahy, and S. A. Basinger
Materials and Components Technology Division
Argonne National Laboratory
9700 South Cass Avenue
Argonne, Illinois 60439

To be presented at *1990 Applied Superconductivity Conf.*, Snowmass Village, CO, Sept. 24-28, 1990. To be published in *IEEE Trans. Magn.*, Vol. 27 (March 1991).

Work at the Argonne National Laboratory was performed under the auspices of the U.S. Department of Energy Superconductivity Pilot Center, Office of Utilities Technologies, Conservation and Renewable Energy, under Contract W-31-109-Eng-38.

Characterization of Composite High Temperature Superconductors for Magnetic Bearing Applications

B. R. Weinberger, L. Lynds, J. VanValzah, H. Eaton
United Technologies Research Center
East Hartford, CT 06108

J. R. Hull, T. M. Mulcahy, S. A. Basinger
Materials and Components Technology Division
Argonne National Laboratory
9700 South Cass Ave, Argonne, IL 60439

Abstract

A study of high temperature superconductor composites for use in magnetic bearings applications is presented. Fabrication and characterization techniques are described. Magnetometry and mechanical force measurements are correlated with a particular emphasis on the role of superconductor particle size. Results are discussed in terms of fundamental limits of Meissner effect levitation.

Proceedings of the 1990 Applied Superconductivity Conference
To be published in IEEE Trans. on Magn. Vol. 27 (Mar 1991)

aa

Introduction

The phenomenon of Meissner effect induced levitation of a permanent magnet above a high temperature superconductor (HTS) at 77 K has evolved from a scientific curiosity with great pedagogical appeal to having real potential for applications in practical rotating machinery. Simple prototype bearings have been fabricated whose rotors are capable of spinning in a stable configuration with minimal friction at high rates of speed [1,2]. Detailed mechanical measurements of the forces between permanent magnets and HTS materials have been performed [3,4]. Levitation pressures and stiffnesses using "conventional" material such as sintered Y-Ba-Cu-O are too small to have practical utility. However, these studies indicate that there is no physical reason that, through the improvement of both the intragranular and intergranular critical current densities (J_c), the pressure and stiffness cannot achieve practical values with Y-Ba-Cu-O [2]. Recent measurements using melt quenched Y-Ba-Cu-O seem to bear this prediction out [5].

Materials requirements for HTS materials to be used in bearing applications are somewhat different from those for other applications such as wires. It has been shown using Y-Ba-Cu-O powder suspended in paraffin [2], that levitation of a magnet can be achieved without a continuous zero resistance path across the superconductor and that the performance of such an insulating matrix HTS composite is equal to that of a cold pressed ceramic HTS material. The mechanical properties of such composites, however, could far exceed those of the brittle ceramics. Mechanical strength of the HTS material could be crucial if the superconductor is to be used as the high speed rotor in a bearing assembly where it may be subject to appreciable centrifugal stresses. Furthermore, the fabrication of the superconductor into large and complicated shapes could be facilitated by a machinable composite matrix or one that could be injection molded. Metal matrix composites could be employed in applications where high thermal conductivity is important. High thermal conductivity could be valuable if the particular application required the superconductor not to be immersed in a cryogenic liquid but cooled by conduction through a cold stage.

This paper describes a study of Y-Ba-Cu-O composites for magnetic bearing applications. Procedures for the fabrication of epoxy matrix and metal matrix composites are described. Measurements of the magnetization versus field and temperature of these composites are presented and correlated with two different mechanical measurements: static force measurements and vibrating beam stiffness measurements. The dependence of levitation properties on the size of the HTS grains in the composite is addressed and discussed in terms of vortex dynamics of a type II superconductor in the mixed state. Finally, the physical limits of Meissner levitation with HTS materials are explored and possible routes to achieve those limits are suggested.

Experimental Details

Samples

All the HTS composites used in this study were based on $YBa_2Cu_3O_{7-x}$. Despite the higher critical temperatures of the Tl and Bi based superconductors, Y-Ba-Cu-O remains the best levitator at 77 K due its superior J_c [4]. The magnitude of the induced magnetization in a type II superconductor in the mixed state is directly related to the size of the supercurrents it can support.

Composites were fabricated using powders processed in different ways to produce differing grain sizes. Calcining under reduced oxygen pressure at 800 C of solid state mixed precursors was used to produce fine powder (≈1 μ) single phase $YBa_2Cu_3O_{7-x}$ [6]. Re-annealing this vacuum calcined material under 1 atm of flowing O_2 at 920 C promoted some grain growth (3-5 μ). $YBa_2Cu_3O_{7-x}$ was also synthesized using precursors co-precipitated out of HNO_3 solution which were sintered, cold pressed and O_2 annealed at 1 atm 920 C. The annealed pellets were reground and yielded material with a broad distribution of grain sizes (≤ 20 μ). $YBa_2Cu_3O_{7-x}/Ag_{1.0}$ synthesized using a similar HNO_3 and co-precipitation route produced material with a more uniform grain size (≈20 μ) [7].

Paraffin composites were fabricated by mixing superconducting powder into melted wax on a hot plate. The resulting mixture was easily moldable into a variety of large shaped objects. This technique produced a composite with approximately a 50% volume fill factor of superconductor which tended to be somewhat non-uniform due to the settling of the powder during solidification.

Epoxy matrix composites were produced by infiltrating pressed pellets of the superconducting powders under vacuum. The pressed pellets made from fully annealed single phase $YBa_2Cu_3O_{7-x}$ powder were immersed in epoxy at 100 C. Infiltration of the epoxy into the pellet was achieved by evacuating the mold containing the pellet and the epoxy. The pumping was maintained until all bubbling due to outgassing ceased. The composite was then cured at 100 C for 10 hours. Void free composites with superconductor volume fraction as high as 70% resulted. An optical micrograph of such a composite made from nitrate co-precipitated $YBa_2Cu_3O_{7-x}$ is shown in Fig. 1. Unlike the wax matrix composites in which the superconducting grains were electrically isolated from each other being completely surrounded by the insulating paraffin, using the vacuum infiltration technique, the macroscopic electrical conduction paths in the pressed

aa

pellets were preserved in the epoxy matrix composites.

Metal matrix composites were formed using finely divided particles of soft metals such as tin and indium. The metal powder was mixed thoroughly with the superconductor powder with a mortar and pestle. The mixture was cold-pressed at 25 ksi. For soft metals, such a pressure was sufficient to produce some flow of the metal around the Y-Ba-Cu-O particles even at room temperature, and at such low temperature no chemical reaction between the Y-Ba-Cu-O and the metals occurred. An optical micrograph of a Y-Ba-Cu-O/Sn (70/30 by volume) composite is shown in Fig. 2. A 3 mm thick pellet of such a metal matrix composite was capable of levitating a permanent magnet without being immersed in liquid nitrogen, thermally sunk to a copper cold stage maintained at 77 K. A paraffin composite of similar dimensions did not have the thermal conductivity to cool sufficiently to levitate the magnet without direct immersion in liquid nitrogen.

Detailed magnetometry and force measurements were performed on the four samples described in Table 1. Three epoxy composites (comp2, comp 1, comp 3) with progressively increasing HTS grain size, and one cold-pressed Y-Ba-Cu-O/Ag ceramic (123/Ag) were studied. The active volume represented the volume of the sample occupied by HTS material. Magnetometry samples were cut as long thin parallelepipeds (0.1 x 0.1 x 1 cm) to minimize demagnetization effects. Force measurements were performed on thin square plates all approximately the same size (1 x 1 x 0.17 cm).

Measurement Techniques

Magnetometry was carried out with a Quantum Design SQUID magnetometer. Magnetization as a function of temperature and field was measured. Minor hysteresis loops with small field excursions (as small as ≈1 gauss) were obtained for comparison to analogous force hysteresis loops. The hysteresis in the field setting of the SQUID superconducting solenoid was checked with a non-hysteretic calibration standard so that the measured hysteresis of the HTS samples was confirmed to originate entirely from the samples.

Static forces between the HTS materials and permanent magnets were acquired using a single pan analytic balance, a repulsive force between the magnet affixed to a pyrex spacer resting on the balance pan and an approaching superconductor indicated by the apparent increase in weight of the magnet. Precise control of the magnet/superconductor separation was achieved using a motorized translation stage. The magnetic field of the permanent magnet as a function of distance was calibrated with a Hall probe gaussmeter.

Dynamic stiffness measurements were obtained using a permanent magnet suspended over the superconductor on a cantilevered beam [7,8]. The motion of the beam was monitored with an Optron optical tracking camera. The dynamic stiffness as a function of oscillation amplitude of the magnet/superconductor system was determined by following the motion of the beam after being plucked, correcting for the dynamic response of the beam itself. By altering the positioning of the beam both horizontal and vertical stiffness could be determined. Static force and dynamic stiffness measurements were performed only at 77 K with the HTS material immersed in liquid nitrogen. However, correlations with magnetometry results permitted the prediction of mechanical performance at low temperatures by using low temperature magnetization data.

Results

Shown in Fig. 3 are representative magnetometry and force results for comp 3, taken at 77 K. Both sets of data were measured while increasing the magnetic field (decreasing the magnet/superconductor separation for the force measurements) following an initial cooldown in zero field. The force data was taken as a function of separation between the HTS composite and a 1.9 cm diameter rare earth permanent magnet which produced a field of 3.4 kgauss at the center of its pole face. Note that in this configuration, for small magnet / superconductor separation, the superconductor experiences a nearly uniform field across its surface pointing perpendicular to the surface. The separation was converted to field strength, so that the data shown is force versus the component of the magnetic field in the levitation direction.

Shown in both the magnetization and force data are minor hysteresis loops at applied fields of 300 and 1000 Gauss obtained by pausing and decreasing the applied field slightly and then returning to the original field. Decreasing the field in the magnetization measurements means lowering the current in the superconducting solenoid, in the force measurement it means increasing the magnet/superconductor separation. The irreversibility associated with vortex pinning is clearly evident in both the force and magnetization results. Previous studies [2,3] have demonstrated that it is the stiffness defined by the slope of the minor force loops ($K = dF/dz$) which determines the mechanical resonant frequency of the coupled magnet / superconductor system, $w = (K/m)^{\frac{1}{2}}$.

A clear correlation between the observed field dependences of the levitation forces and magnetization can be demonstrated. Consider a point magnetic dipole arising from a superconductor, μ, oriented along the z axis in a magnetic field H. The potential energy of such a dipole is $-\mu \cdot H$. It should be kept in mind that $\mu = \mu(H)$. The levitation force

aa

felt by the dipole is in the z direction and is given by the negative gradient of the energy,

$$F = (\mu + H d\mu/dH)\, dH/dz \qquad (1)$$

For a type I superconductor $\mu = HV/(4\pi)$, where V is the volume of the superconductor, so that the force is given by,

$$F = \frac{HV}{2\pi}(dH/dz) = 2\mu\,(dH/dz) \qquad (2)$$

For type II superconductors equation (2) is valid for fields less than Hc1 or even somewhat larger if there is strong flux pinning. However, at high fields, with the superconductor in the mixed state equation (1) applies.

Compared in Fig. 4 are levitation force data measured with the analytical balance, and forces derived from magnetometry data using equation (1). $\mu(H)$ and $d\mu/dH$ were obtained from SQUID magnetometry results and dH/dz from measured magnetic field versus distance data for the permanent magnet used in the force measurements. The magnet was assumed to produce a field in the z direction, uniform in the xy plane and demagnetization effects on both the permanent magnet and the superconductor were ignored. Considering these assumptions the agreement between the measured force data and the data derived from the magnetometry results is striking.

Levitation Pressure

Fig. 5 displays the 77 K zero field cooled levitation force data for the four samples listed in Table 1. Fig. 6 shows the corresponding 77 K magnetization data. The magnetization data in Fig. 6 is normalized to the actual volume of superconductor in each sample (see Table 1). Clearly, as predicted by equations (1) and (2), for a given applied field the magnitude of the levitation force increases with the size of the field induced magnetization.

Also noteworthy in Figs. 5 and 6 is that at low fields, both the magnetization and levitation force scale with the HTS crystallite size. This dependence is attributable to penetration depth effects. Small particle composites (such as comp 2), with grain sizes of the order a few times the London penetration depth (≈ 2000 Å at 77 K for $YBa_2Cu_3O_x$)[9,10] will experience field penetration into an appreciable fraction of each superconducting grain and consequently yield a drastically smaller Meissner moment than larger grain composites, even at fields less than H_{c1}. This grain size dependence implies that the screening currents which produce the observed magnetization and levitation forces are intragranular even though intergranular conduction paths exist in the epoxy matrix composites. The existence of large

00

size screening current loops is undoubtedly limited by low critical current weak links across grain boundaries. The largest grain sample (123/Ag) had large enough grains that the penetration represented a negligibly small fraction of the volume of each grain so that at low fields the magnetization approached 100 % flux exclusion, $M = [-1/4\pi] H$.

Interestingly, the magnetization of and the levitation forces from the small grain samples are comparable to that of the large grain (123/Ag) sample at higher fields. In fact, the largest levitation force at fields in excess 300 gauss were generated by comp 2, which had significantly smaller grains than either comp 3 or 123/Ag. It therefore can be misleading to qualify materials according to the heights at which they levitate magnets. At large heights, the magnetic fields are quite low and the larger grain samples of the group studied would out-perform the smaller grained sample. However, at larger more technologically relevant fields of a few kgauss, such as is easily produced close to a permanent magnet, the advantage of the large grained material in terms of levitation pressure disappears.

The origin of the larger magnetization of the small grain composites at high fields may lie in surface barriers to the entry of vortices. Vortices will be repelled by other vortices as well as the magnetic field in the London penetration layer [11]. In small grains where individual vortices cannot isolate themselves from either of these influences, it may be energetically favorable for flux to be inhibited from penetration into the grains at fields well past H_{c1}. Without flux penetration the Meissner moment and hence the levitation force continues to increase with field.

In addition to the effects of the London penetration volume and surface barriers to flux entry, there is a third way in which grain size could effect magnetization in a composite HTS material via bulk pinning of vortices. The bulk pinning of vortices controls the intragranular J_c, and its effect upon magnetization can treated in terms of a critical state model. Consider a composite formed f[illegible] an array of cylindrical particles, radius R, height L, with intergranular J_c of zero and an external field applied parallel to the axis of the cylinders. Following the Bean critical state model [12], assuming a field independent J_c, the maximum magnetization of such a sample will be produced when the applied field reaches a value H^*.(For a slab of thickness D, $H^* = \pi J_c D/5$ with H^* in gauss and J_c in A/cm^2.) Further increases in field will produce no increases in magnetization. The superconductor is said to be in the "critical state" in which screening supercurrents circulate around the grains, everywhere with a density J_c. The magnetic moment of each cylindrical grain in the critical state is therefore,

$$\mu_{max} = \int_0^R \pi r^2 J_c Ldr = \pi J_c LR^3/3 \qquad (3)$$

To get the magnetization of such a composite, equation [3] is divided by the volume of the cylindrical grains, $\pi R^2 L$.

$$M_{max} = J_c R/3 \qquad (4)$$

Therefore, to maximize the induced magnetization and thereby the levitation pressure in a composite superconductor, it is necessary to maximize the product $J_c R$. This effect of the dependence of magnetization on the size of the supercurrent loops has been demonstrated by scribing high quality thin films [13]. Among the four samples studied, there was clearly a trade-off among penetration volume, current loop size, and surface barrier effects best met by grains of intermediate size (comp 1).

The 77 K magnetization data in Fig. 6 is instructive in that the deficiencies of the sintered Y-Ba-Cu-O used in this study are apparent and the achievable limits clearly delineated. The maximum possible diamagnetic response of a superconductor is 100 % flux exclusion shown in Fig. 6 by the line labelled $-M = (1/4\pi)H$. At 77 K and practical fields of 3000 gauss, these materials produced a Meissner moment of only a few percent of complete flux exclusion. With stronger flux pinning or surface barriers, vortices could be inhibited from entering the superconductor until much higher fields, increasing the magnetization and the levitation pressures produced. The sintered Y-Ba-Cu-O used in this work produce levitation pressures of ≈0.2 psi on 3 kgauss permanent magnets at 77 K. Clearly, there is no fundamental physical reason why pressures of 10 psi are not achievable and with higher magnetic fields with enhanced field gradients perhaps significantly higher pressures may be reached.

While the operation of a HTS superconducting bearing at 77 K or higher presents clear engineering and cost advantages through the use of liquid nitrogen as the cryogen, there may be performance advantages to be gained at lower temperatures. In certain potential applications, such as turbomachinery for liquid hydrogen fueled rocket engines, working environments with temperatures of 20 K already exist. The correlation between the magnetometry and force data shown in Figs. 4-6 leads to confidence that low temperature magnetometry measurements may be used to predict mechanical force behavior at low temperatures where force measurements are not straightforward.

Shown in Fig. 7 are magnetization versus field data (zero field cooled) at 20 K for the four test samples characterized in Figs. 4-6. It is notable that for each material, the peak in the magnetization has moved to higher field, and at 3000 gauss, each is ten times larger than its corresponding value at 77 K. What may be inferred, then, are levitation pressures also a factor of ten larger than what was measured at 77 K, levitation pressures at 20 K of 2-3 psi. Several effects could be influencing this low temperature improvement. There is an decrease in the London penetration depth at low temperatures evidenced in the larger low field magnetization of the small particle sample (comp 2). Depinning of vortices and the overcoming of surface barriers can be a thermally activated process so that increased magnetization would be expected for each sample. Nevertheless, at 3000 gauss and 20 K, there is still room for another factor of five improvement before the 100 % Meissner effect limit is reached.

Vertical Magnetic Stiffness

The stiffness is an important design parameter in any bearing system. It may be defined for a given direction **r**, by $K_r = dF_r/dr$ which quantifies the restoring force experienced by a levitated magnet when disturbed from its equilibrium position. K also determines the natural frequencies of the vibrational modes of levitated components. In designs of high speed rotating machinery precisely defined equilibrium positions, critical frequencies, and control of the normal modes are crucial as is the ability to withstand transient perturbations.

Of primary importance is the vertical stiffness, $K_z = dF/dz$, the stiffness in the levitation direction. Differentiation of equation (1) predicts that K_z will depend both on the magnitude of the induced magnetic moment, μ, and its first two derivatives with respect to field, $d\mu/dH$ and $d^2\mu/dH^2$.

$$K = \mu\, d^2H/dz^2 + d\mu/dH\, [\, H\, d^2H/dz^2 + 2\, (dH/dz)^2\,] + d^2\mu/dH^2\, [\, H\, (dH/dz)^2\,] \qquad [5]$$

With the hysteretic behavior of type II superconductors in the mixed state, it is not immediately obvious which magnetization slope, $d\mu/dH$, is involved, that of the major magnetization curve or the minor loop in Fig. 3. Previous static force and vibration studies of permanent magnet / HTS systems have demonstrated that it is the slope of the minor force loops (such as those shown in Fig. 3) which determine the dynamic response of the coupled mechanical system.

Shown in Fig. 8 are 77 K vertical stiffness data for three of the test samples as a function of vibration amplitude using the plucked beam technique. The magnet/superconductor separation was chosen so that the field at the surface of the superconductor was approximately 1000 gauss. The smallest grain composite (comp 2) yielded a stiffness too small to separate from that of the bare beam. In Fig. 9 are plotted the slopes (dM/dH) of the magnetization loops (like those of Fig. 3) as a function of the amplitude of the excursion from H_o = 1000 gauss. Analogous behavior to the mechanical stiffness data in Fig. 8 is evident. Therefore, for the experimental configuration used to obtain the data of Fig. 8 , the second term in equation (6), that proportional to $d\mu/dH$ is apparently quite important. For H_o = 1000 gauss and low vibration amplitudes (field excursions) the stiffest sample was Y123/Ag which was not the sample yielding the largest magnetization and levitation pressure (comp 1). The previously observed empirical rule that stiffness scales with levitation pressure is not universally valid.

The slopes of the minor magnetization hysteresis loops (Fig. 9), which strongly influence the mechanical stiffness, are also clearly correlated with the low field Meissner fractions (Fig. 6) for the samples studied. The samples with the largest low field flux exclusion also produce minor loops with the largest slopes, at least for small excursions δH. This parallel argues that the vibrational behavior in the vertical direction is largely due to the dynamic response of that part of the superconductor's magnetization arising from the surface screening currents. Due to London penetration depth effects, samples with the largest grains have the largest total screening currents flowing and consequently are mechanically stiffest. As their amplitudes increase, however, the minor loops become more hysteretic indicating the onset of vortex motion. Such a model also explains the more drastic decrease in both the mechanical (Fig. 8) and magnetic stiffness (Fig. 9) with amplitude for the largest grain sample (123/Ag). As already suggested, such large particles can accommodate larger vortex densities due to minimized inter-vortex and surface barrier repulsive effects and so are most susceptible to flux motion. However, vortex dynamics must play some role in the vertical stiffness even at low vibration amplitudes. For the largest grain samples at low amplitudes, at 77 K and H_o = 1000 gauss, dM/dH does not achieve the pure Meissner screening current value of $1/4\pi$.

As with the levitation pressure results, comparison between the magnetic and mechanical stiffness results can provide insight as to the physical limits to which the stiffness can be pushed. As alluded to above, the limiting slope dM/dH at which the screening currents can respond is the complete Meissner effect limit $1/(4\pi)$ = 0.080. As may be seen in Fig. 9, at 77 K , H_o = 1000 gauss, and δH = 5 gauss, the maximum magnetic stiffness measured was 0.025 for the 123/Ag sample. As with the levitation pressure these values improve at 20 K, again presumably due to improved vortex pinning. These results are shown in Fig. 10. At low temperatures the theoretical limit of 0.08 is being approached by the 123/Ag sample.

Horizontal Magnetic Stiffness

If the forces between a magnet and a type I superconductor with a horizontal flat surface are modelled in terms of those between a magnet and an image magnet in the superconductor, clearly there will be only forces in the vertical direction. Neglecting edge effects, there will be no horizontal restoring forces or stiffness. The lack of a horizontal restoring force prompted early experimenters to employ a bowl shaped superconductor to achieve stable levitation [14]. For a type II superconductor in the mixed state, however, horizontal motion of the suspended magnet implies the movement of vortices within the superconductor, out of some regions, into others. Therefore, if internal vortex pinning is appreciable, there will be barriers opposing horizontal deflection [15]. The image of the suspended magnet in the superconductor may be distorted in the direction of the horizontal motion resulting in magnetic forces on the suspended magnet opposing such motion. The dissipation associated with the irreversibility of vortex motion will manifest itself as a viscous drag [16]. Such vortex drag effects may be easily demonstrated by spinning a levitated magnet above a superconductor. If the magnet's field is cylindrically symmetric about its axis of rotation, it will spin freely. If it is even slightly asymmetric *magnetically* about its axis of rotation, its rotational energy will rapidly dissipate.

Horizontal stiffness measurements were performed for each of the samples in Table 1 using the plucked beam technique with the displacement of the beam, and the magnet attached to it, parallel to the superconductor surface. The pole face of the magnet employed was comparable in dimension to the HTS samples. Therefore edge effects may not have been negligible. Nevertheless, the results are qualitatively similar to those obtained with a magnet substantially smaller in area than the superconductor [8]. The dependence of the horizontal stiffness on amplitude is shown in Fig. 11. A comparison of Figs. 8 and 11 reveals that for each sample, for the same magnet/superconductor separation and vibration amplitude, the vertical stiffness was a factor of three larger than the horizontal. The lack of a Meissner screening current contribution to the horizontal stiffness, present in the vertical case, accounts for the smaller horizontal mechanical stiffness.

The sample dependence of the horizontal stiffness behavior shown in Fig. 11 is similar to that of the vertical stiffness in Fig. 8, but for different reasons. The vertical stiffness dependence on grain size was explicable by a London penetration depth argument, the larger grains containing more integrated screening current and consequently producing more of a vertical spring constant. The greater horizontal stiffness of the large grain samples may be attributable to the greater density of pinned vortices in the large grains. Due to their surface barriers, few vortices can enter the small grain samples which consequently more closely approximate the reversible behavior of a type I superconductor which produces no horizontal stiffness.

The horizontal stiffness results provide further insight into the magnetic behavior of HTS materials which leads to the observed mechanical behavior of the coupled magnet/HTS system. Though, from a practical design point of view, the horizontal stiffness is of secondary importance. Any practical superconductor bearing design would not employ flat planar bearing surfaces but rather suitably shaped superconducting components so that the horizontal stiffness actually results from a "vertical" stiffness turned sideways. An example of such a shape would be a U or a bowl shape.

Conclusions

Several important conclusions can be drawn from the experimental results presented in the preceding section. The principal conclusion to be drawn addresses the practical utility of HTS composites in magnetic levitation applications. HTS composites, both insulating and metal matrix, represent a realistic alternative to ceramic HTS materials for magnetic levitation applications at temperatures as high as 77 K. They can satisfy requirements of mechanical strength, machinability, and thermal conductivity unique to rotating machinery applications without sacrificing load bearing or stiffness capabilities.

The results, however, show that there is substantial room for improvement of the superconducting properties of the HTS material, specifically in critical currents, if the full potential of HTS Meissner effect levitation is to be realized. Magnetometry measurements coupled with mechanical force and stiffness measurements clearly delineate these limits. Levitation pressures in excess of 10 psi are achievable using 3 kgauss permanent magnets if the crystallite size and flux pinning can be improved. Recent breakthroughs in HTS materials synthesis involving melt processing producing material with impressive magnetization properties [17-20] demonstrate that such improvements are possible.

The 77 K stiffness data in Fig. 8 level out at about 1 lb/in, for a 1 cm^2 bearing surface area, to small to be of any practical value. However, substantial improvements in these values are allowed by the limits imposed by a more complete Meissner effect: μ, $d\mu/dH$ $d\mu/dH$ in equation (5). Furthermore, the stiffness scales with the area of the bearing surface making possible much stiffer bearings if machinery designs could be adjusted to tolerate larger bearing surface areas.

One important factor in controlling the superconducting properties of an HTS composite is the HTS crystallite size. Conflicting effects of particle size were identified by scrutinizing magnetometry results. Small particle composites had their net magnetization and resultant levitation pressure limited by London penetration of externally applied fields, yet at high fields produced magnetizations as great or greater than the larger particle composites because of superior resistance to vortex penetration. Larger particle composites benefitted from the larger size of the screening current loops producing larger magnetization and the larger net screening currents producing a greater vertical stiffness, but suffered from a greater susceptibility to flux penetration and vortex movement which limited the high field levitation pressures and lowered the magnetic stiffness for large amplitude vibrations. Optimized composites will therefore represent a compromise among several competing factors. Although, unambiguously, improved performance will be produced by strongly pinned, high J_c material.

Much remains to be accomplished in improving HTS magnetic bearing performance by improvement of HTS superconducting properties. Even further potential performance gains may be effected by innovative design approaches. Equations (1)] and (5) suggest design considerations which as yet have not been seriously addressed. Improved levitation pressure and stiffness will be produced by maximizing not only H, but dH/dz and d^2H/dz^2 as well. Thus improved performance will be brought about by appropriately shaping the superconductor and the magnetic field of the magnet.

All published work to date has employed permanent magnets. Such magnets limit the operational fields to a few kgauss. Clearly higher magnetic fields would produce enhanced magnetization, levitation pressure, magnetic stiffness, particularly if the superconducting properties of the HTS material is also improved. Fields much larger than that attainable using permanent magnets can be created using superconducting solenoids. A potential novel approach for generating high fields could be the use of trapped flux HTS magnetic "replicas". Actual trapped flux HTS magnets have already been produced with captured fields exceeding 1 kgauss [21]. Ultimately, the practicality of HTS magnetic bearings certainly will hinge on such novel engineering approaches.

Acknowledgments

The technical assistance of R. Boddurtha and S. Sheades (UTRC) is gratefully recognized. Work at Argonne National Laboratory was performed under the auspices of the U. S.

Department of Energy, Conservation and Renewable Energy, Superconductivity Pilot Center, under Contract W-31-109-Eng-38.

References

1. F. C. Moon and P. -Z. Chang, "High-speed rotation of Magnets on high T_c superconducting bearings", *Appl. Phys. Lett.* 56, 397 (1990).

2. B. R. Weinberger, L. Lynds and J. R. Hull, "Magnetic bearings using high-temperature superconductors: some practical considerations", *Supercond. Sci. Technol.* 3, 381 (1990).

3. F. C. Moon, M. M. Yanoviak and R. Ware, "Hysteretic levitation forces in superconducting ceramics", *Appl. Phys. Lett.* 52, 1534 (1988).

4. P. -Z. Chang, F. C. Moon, J. R. Hull and T. M. Mulcahy, "Levitation force and magnetic stiffness in bulk high-temperature superconductors", *J. Appl. Phys.* 67, 4358 (1990).

5. F. -C. Moon, P. -Z. Chang, H. Hojaji and A. A. Thorpe, "Levitation forces, relaxation and magnetic stiffness of melt-quenched $YBa_2Cu_3O_x$", *Jap. J. Appl. Phys.* (preprint).

6. U. Balanchandran, R. B. Poeppel, J. E. Emerson, S. A. Johnson, M. T. Lanagan, C. A. Youngdahl, D. Shi and K. C. Goretta, "Synthesis of phase-pure orthorhombic $YBa_2Cu_3O_x$ under low oxygen pressure", *Mater. Lett.* 8, 454 (1989).

7. B. R. Weinberger, L. Lynds, D. M. Potrepka, D. B. Snow, C. T. Burila, H. E. Eaton, R. Cipoli, Z. Tan and J. I. Budnick, "Y-Ba-Cu-O/Silver composites: an experimental study of microstructure and superconductivity ", *Physica C* 161, 91 (1989).

8. S. A. Basinger, J. R. Hull and T. M. Mulcahy, "Amplitude dependence of magnetic stiffness in bulk high-temperature superconductors", *Appl. Phys. Lett.* (preprint).

9. D. R. Harshman, G. Aeppli, E. J. Ansaldo, B. Batlogg, J. H. Brewer, J. F. Carolan, R. J. Cava, M. Celio, A. C. Chaklader, W. N. Hardy, S. R. Kreitman, G. M. Luke, D. R. Noakes and M. Senba, "Temperature dependence of the magnetic penetration depth in the high temperature superconductor $Ba_2YCu_3O_{9-\delta}$: evidence for conventional s-wave pairing", *Phys. Rev. B* 36, 2386 (1987).

10. L. Krusin-Elbaum, R. L. Greene, F. Holtzberg, A. P. Malozemoff and Y. Yeshurun, "Direct measurement of the temperature-dependent magnetic penetration depth in Y-Ba-Cu-O crystals", *Phys. Rev. Lett.* 62, 217 (1989).

11. C. P. Bean and J. D. Livingston, "Surface barrier in type-II superconductors", *Phys. Rev. Lett.* 12, 15 (1964).

12. C. P. Bean, "Magnetization of hard superconductors", *Phys. Rev. Lett.* 8, 250 (1962).

13. B. Oh, M. Naito, S. Arnason, P. Rosenthal, R. Barton, M. R. Beasley, T. H. Geballe, R. H. Hammond and A. Kapitulnik, "Critical current densities and transport in superconducting $YBa_2Cu_3O_{7-\delta}$ films made by electron beam co-evaporation", *Appl. Phys. Lett.* 51, 852 (1987).

14. V. Arkadiev, "A floating magnet", *Nature* 160, 330 (1947).

15. L. C. Davis, "Lateral restoring force on a magnet levitated above a superconductor", *J. Appl. Phys.* 67, 2631 (1990).

16. E. H. Brandt, "Friction in levitated superconductors", *Appl. Phys. Lett.* 53, 1554 (1988).

17. M. Murakami, M. Morita, K. Doi and K. Miyamoto, "A new process with the promise of high J_c in oxide superconductors", *Jap. J. Appl. Phys.* 28, 1189 (1989).

18. M. Murakami, S. Gotoh, N. Koshizuki, S. Tanaka, T. Matsushita, S. Kambe and K. Kitazawa, "Critical currents and flux creep in melt processed high T_c oxide superconductors", *Cryogen.* 30,390 (1990).

19. S. Jin, R. C. Sherwood, E. M. Gyorgy, T. H. Tiefel, R. B. van Dover, S. Nakahara, L. F. Schneemeyer, R. A. Fastnacht and M. E. Davis, "Large magnetic hysteresis in a melt-textured Y-Ba-Cu-O superconductor", *Appl. Phys. Lett.* 54, 584 (1989).

20. H. Hojaji, A. Barkatt, K. A. Michael, S. Hu, A. N. Thorpe, M. F. Ware, I. G. Talmy, D. A. Haught and S. Alterescu, "Yttrium enrichment and improved magnetic properties in partially melted Y-Ba-Cu-O materials", *J. Mater. Res.* 5, 721 (1990).

21. R. Weinstein, I. -G. Chen, J. Liu, D. Parks, V. Selvamanickam and K. Salama, "Pesistent magnetic fields trapped in high T_c superconductor", *Appl. Phys. Lett.* 56, 1475, (1990).

TABLE I

Test Samples

Name	Superconductor Material	Crystallite Size	Active Volume
Comp 2	$YBa_2Cu_3O_x$ vacuum calcined	≈ 1 μm	59%
Comp 1	$YBa_2Cu_3O_x$ vacuum calcined re-annealed	≈ 3-5 μm	68%
Comp 3	$YBa_2Cu_3O_x$ HNO_3 precipitated	≈ 2-25 μm	66%
123/Ag	$YBa_2Cu_3O_x/Ag_1$ HNO_3 precipitated cold-pressed ceramic	≈ 20 μm	85%

AS REC'D
500X

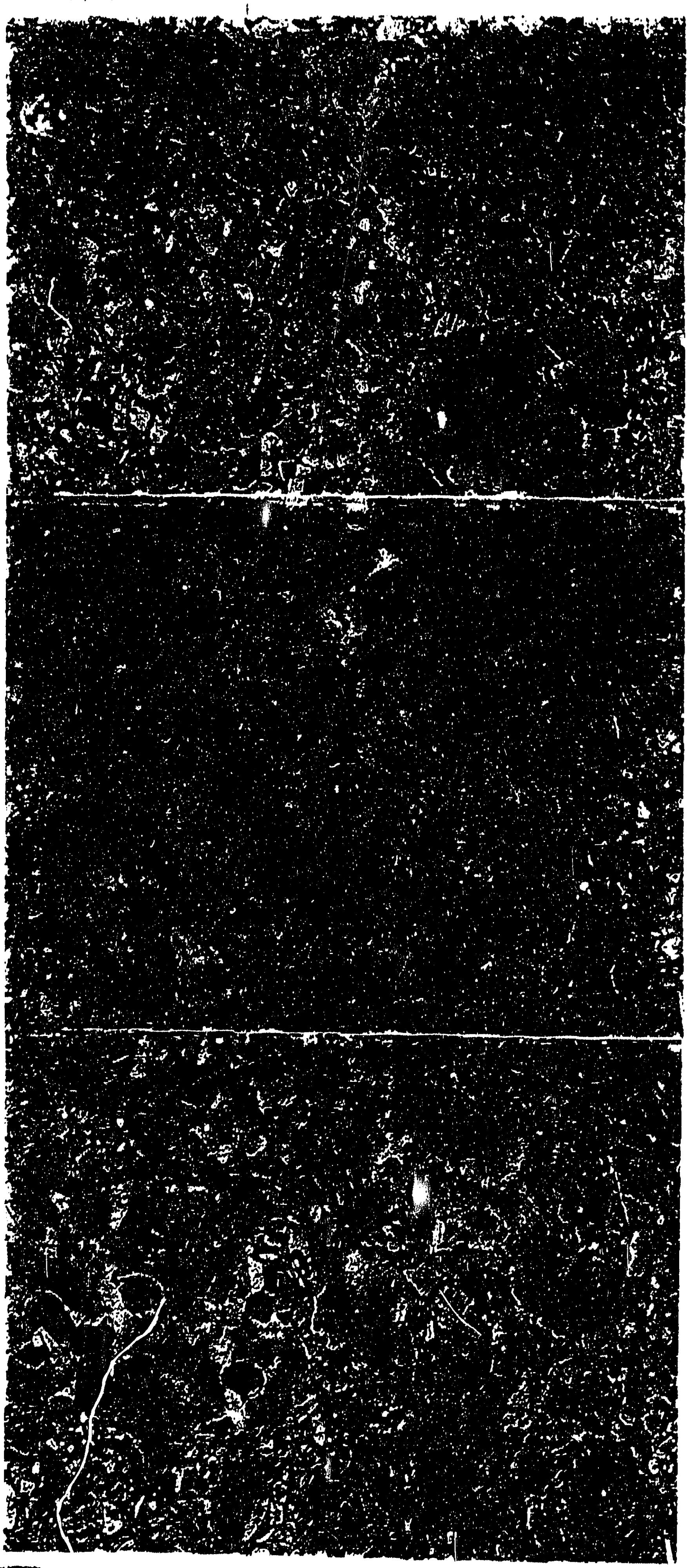

20 μ

Fig. 1

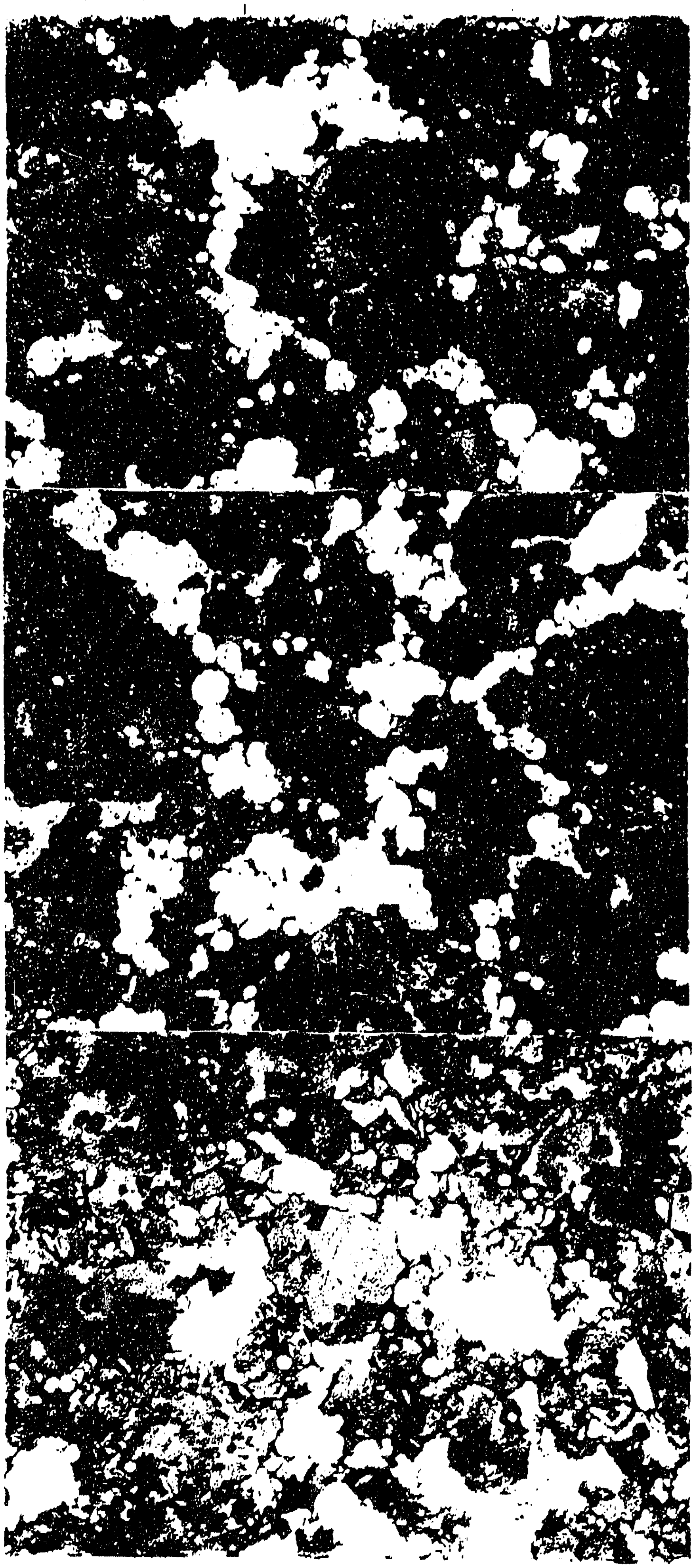

20μ

Fig 2

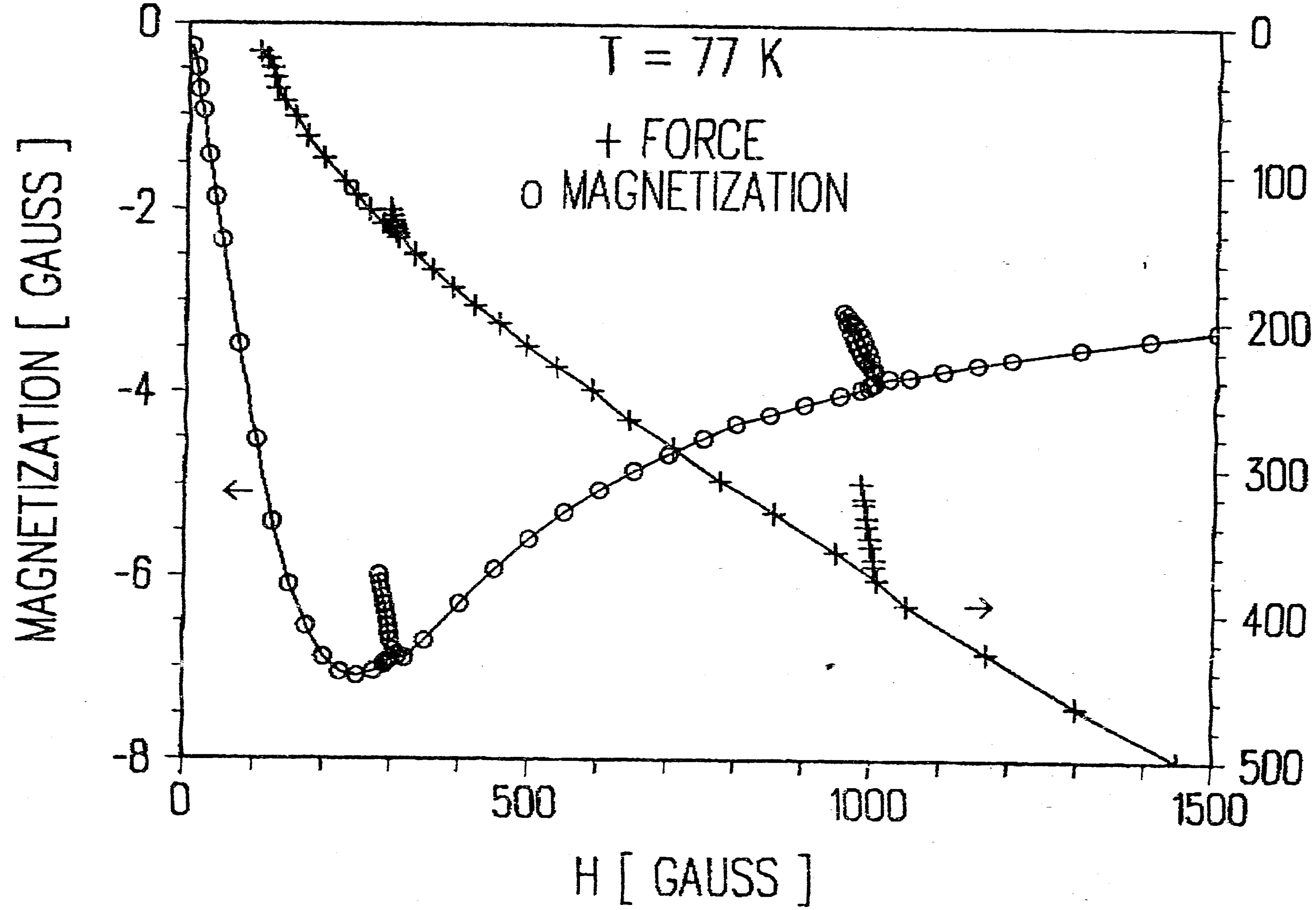
T = 77 K
+ FORCE
o MAGNETIZATION
MAGNETIZATION [GAUSS]
0
-2
-4
-6
-8
FORCE [DYNES]
0
100
200
300
400
500
H [GAUSS]
0
500
1000
1500

FIG. 3

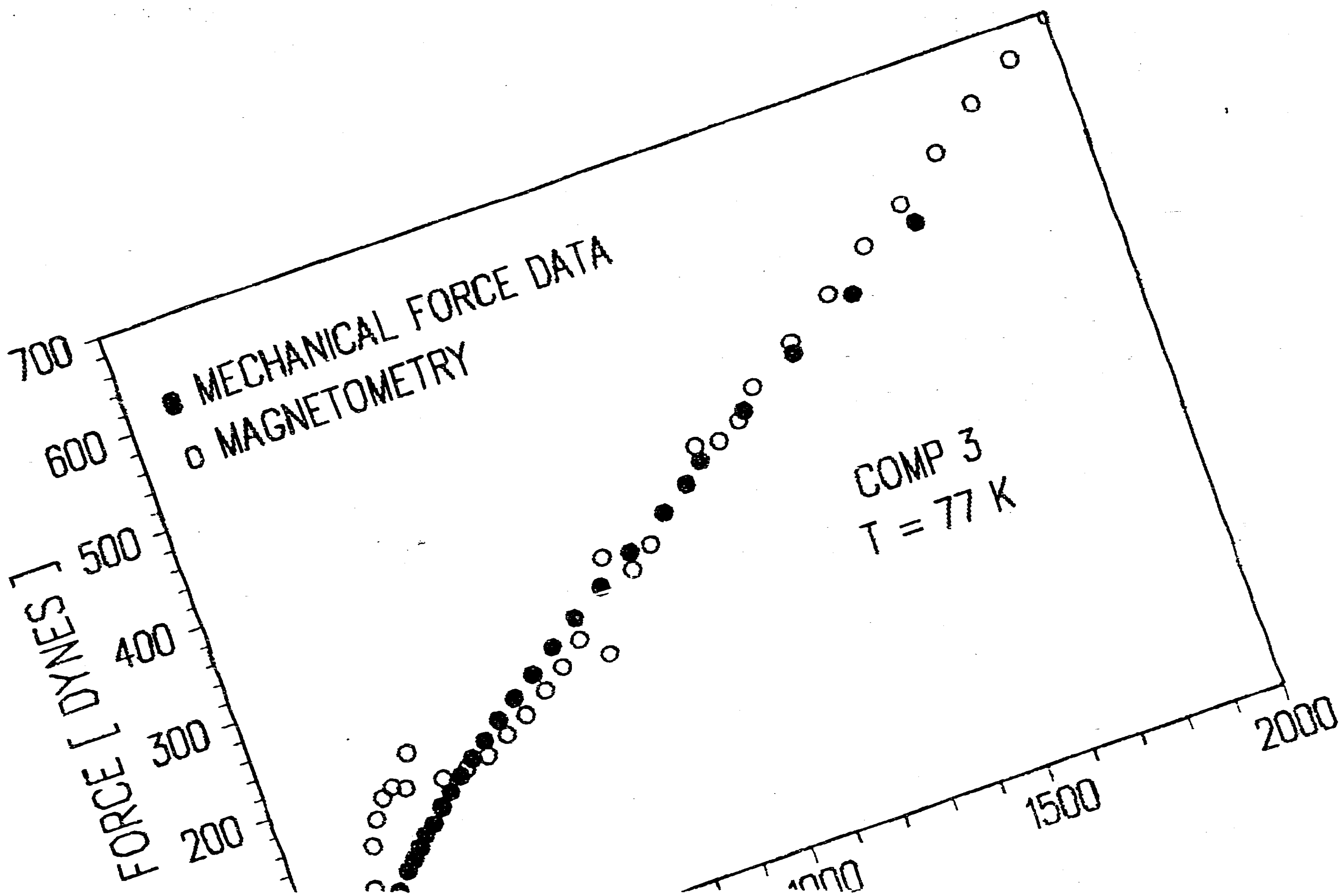

● MECHANICAL FORCE DATA
o MAGNETOMETRY
COMP 3
T = 77 K
FORCE [DYNES]
700
600
500
400
300
200
2000
1500

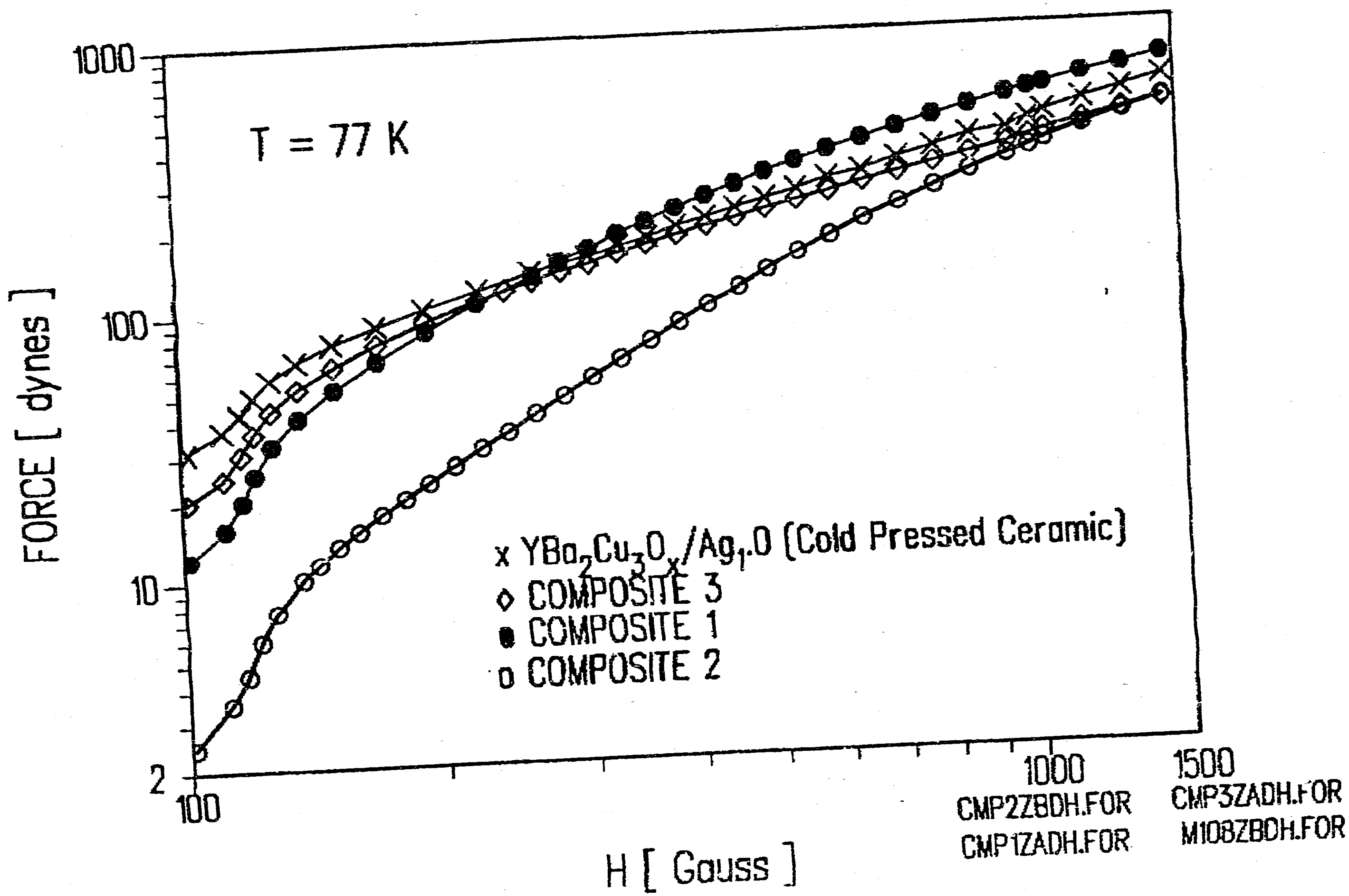
T = 77 K
FORCE [dynes]
1000
100
10
2
100
1000
1500
H [Gauss]
x $YBa_2Cu_3O_x/Ag_1.0$ (Cold Pressed Ceramic)
◇ COMPOSITE 3
● COMPOSITE 1
o COMPOSITE 2
CMP2ZBDH.FOR
CMP1ZADH.FOR
CMP3ZADH.FOR
M108ZBDH.FOR

FIG 5

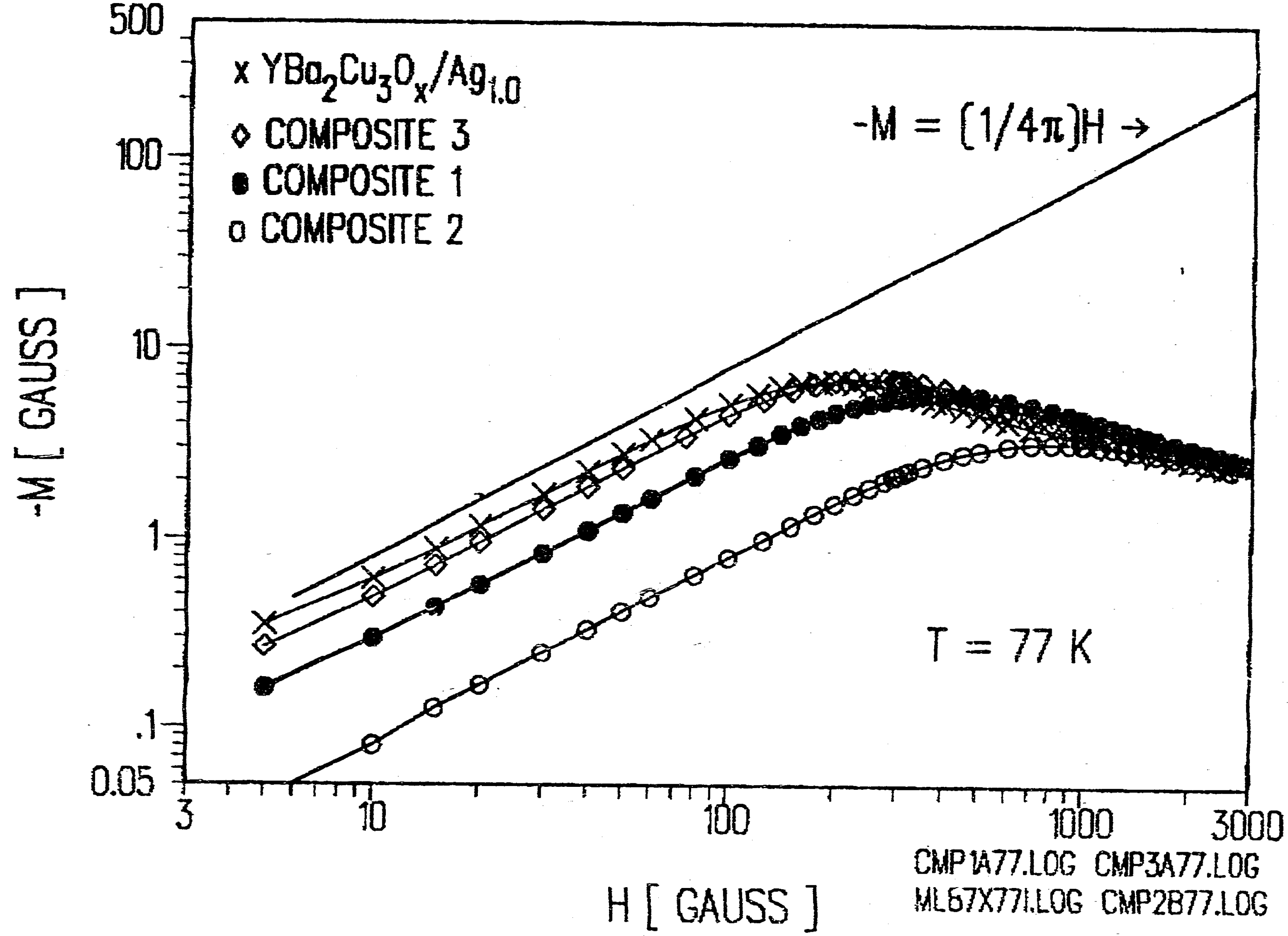

x YBa2Cu3Ox/Ag1.0
◇ COMPOSITE 3
● COMPOSITE 1
○ COMPOSITE 2
-M = (1/4π)H →
T = 77 K
-M [GAUSS]
500
100
10
1
.1
0.05
3
10
100
1000
3000
H [GAUSS]
CMP1A77.LOG CMP3A77.LOG
ML67X77I.LOG CMP2B77.LOG

Fig 6

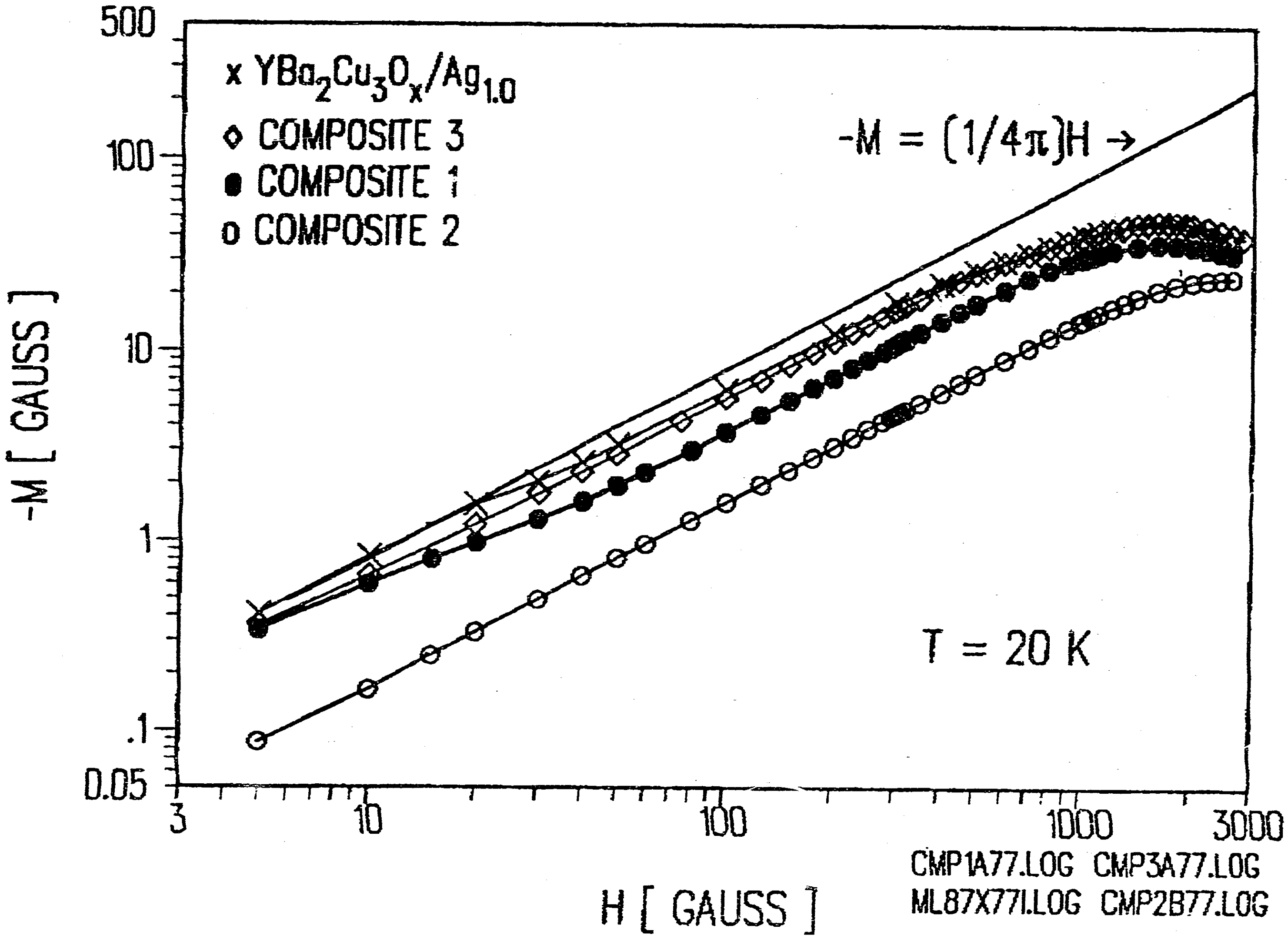
x $YBa_2Cu_3O_x/Ag_{1.0}$
◇ COMPOSITE 3
● COMPOSITE 1
o COMPOSITE 2
$-M = (1/4\pi)H$ →
T = 20 K
-M [GAUSS]
H [GAUSS]
500
100
10
1
.1
0.05
3
10
100
1000
3000
CMP1A77.LOG CMP3A77.LOG
ML87X77I.LOG CMP2B77.LOG

Fig 7

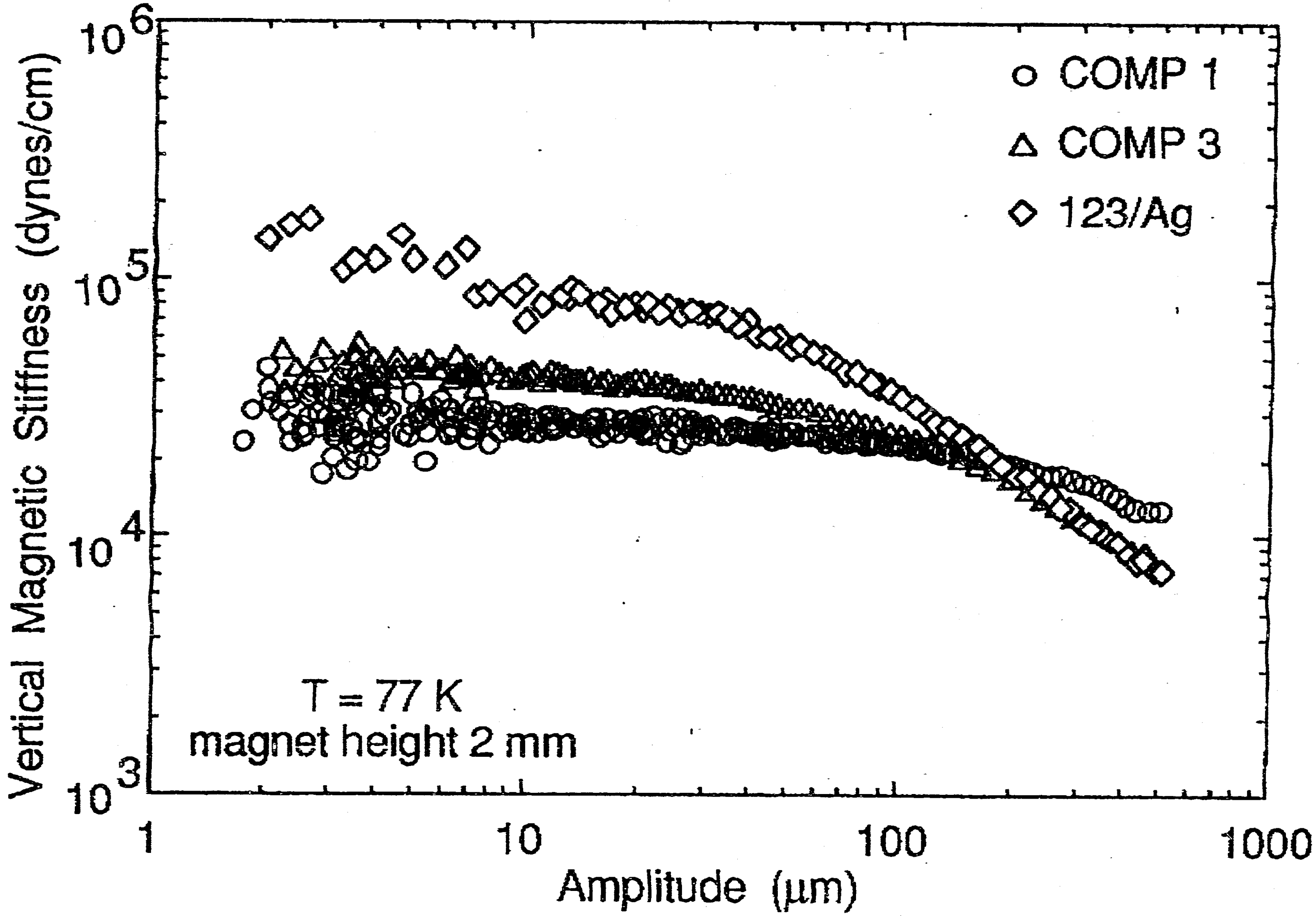

Vertical Magnetic Stiffness (dynes/cm)
10^6
10^5
10^4
10^3
1
10
100
1000
Amplitude (μm)
COMP 1
COMP 3
123/Ag
T = 77 K
magnet height 2 mm

Fig 8

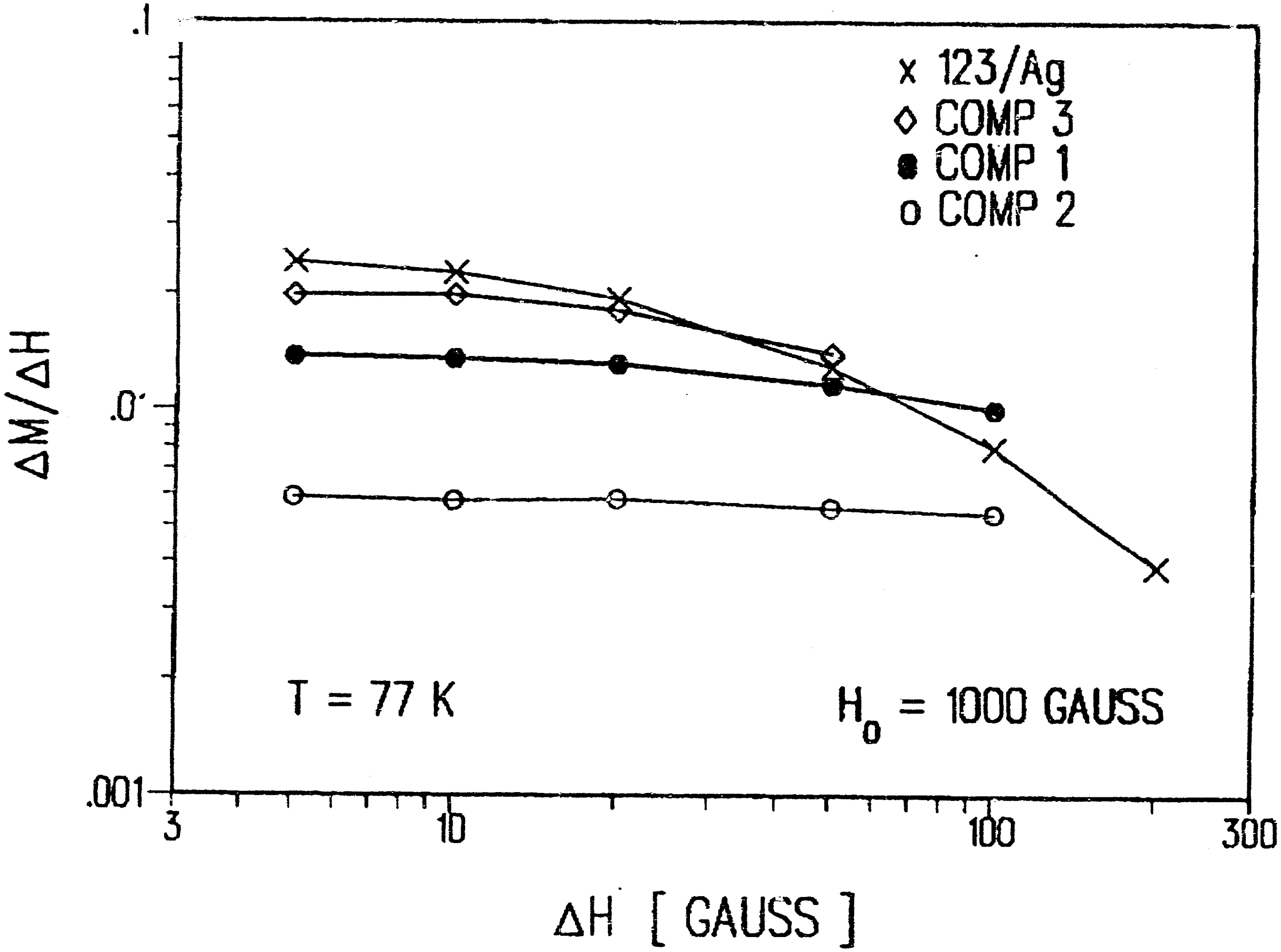
x 123/Ag
◇ COMP 3
● COMP 1
o COMP 2
ΔM/ΔH
.1
.01
.001
3
10
100
300
T = 77 K
H0 = 1000 GAUSS
ΔH [GAUSS]

Fig 9

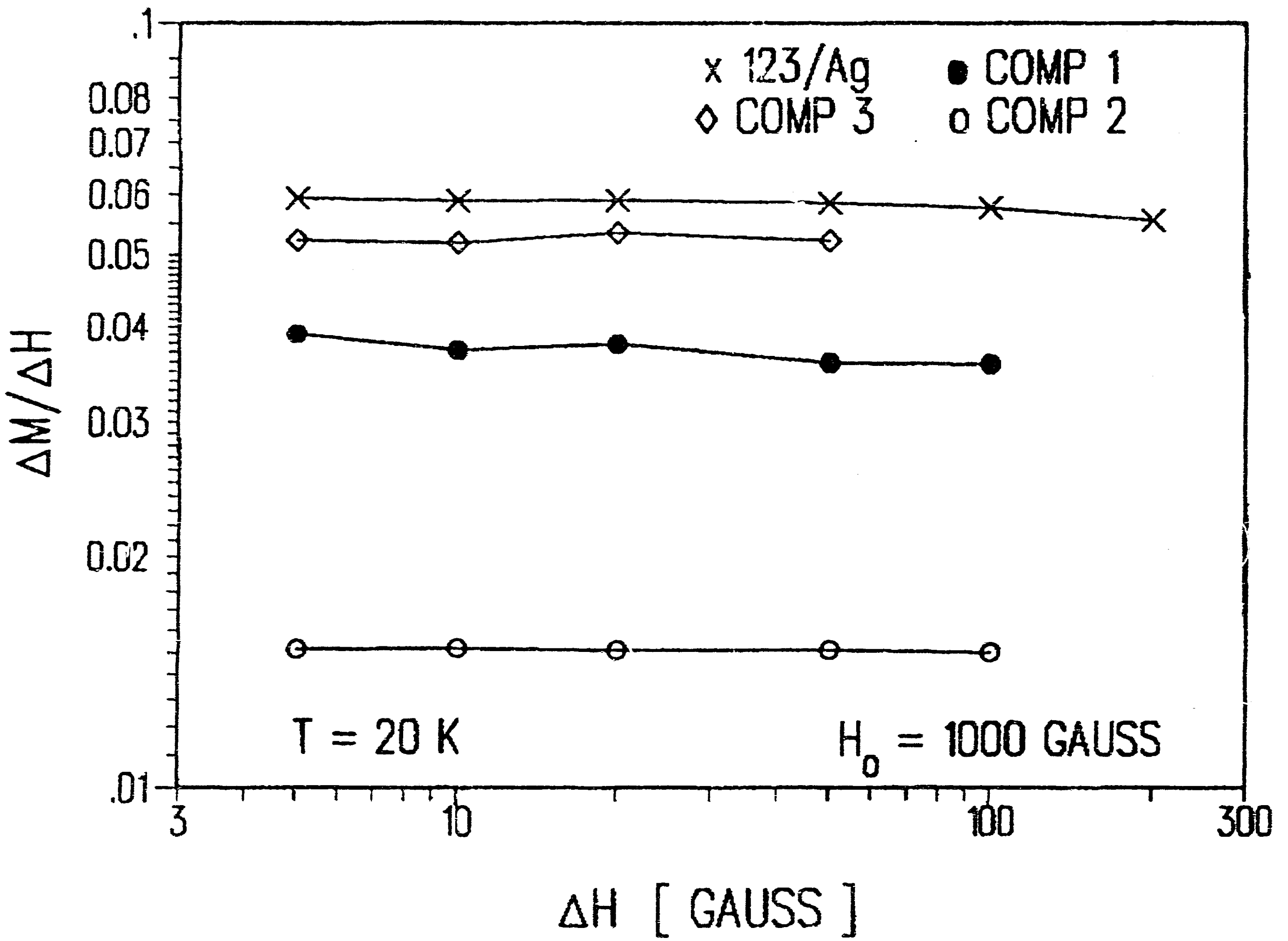
x 123/Ag
● COMP 1
◇ COMP 3
o COMP 2
T = 20 K
H_o = 1000 GAUSS
ΔM/ΔH
.1
0.08
0.07
0.06
0.05
0.04
0.03
0.02
.01
3
10
100
300
ΔH [GAUSS]

Fig. 10

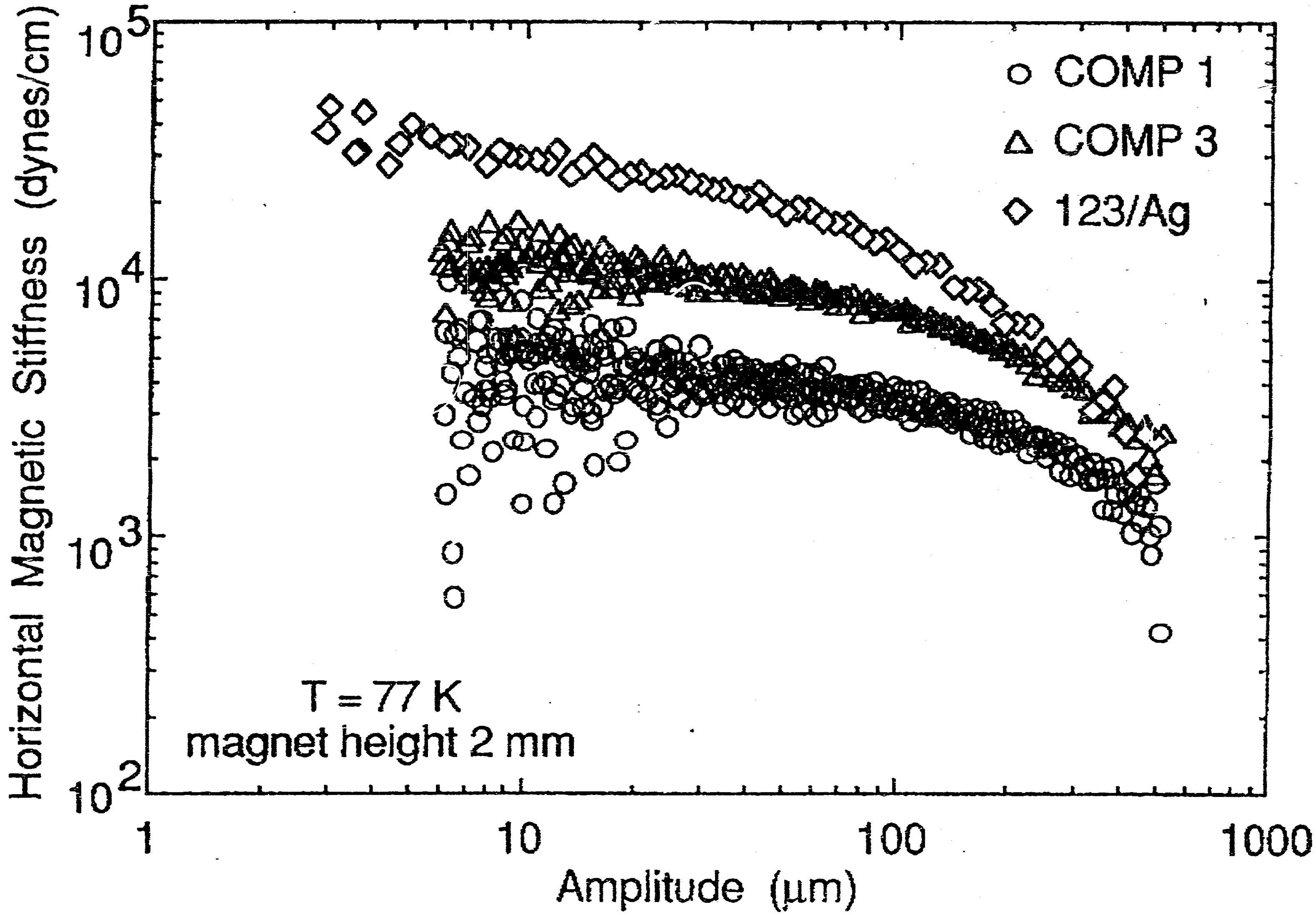

Horizontal Magnetic Stiffness (dynes/cm)
10^5
10^4
10^3
10^2
1
10
100
1000
Amplitude (µm)
COMP 1
COMP 3
123/Ag
T = 77 K
magnet height 2 mm

Fig 11

END

DATE FILMED

02 / 05 / 91